Liquid droplet spreading with line tension effect

2006 J. Phys.: Condens. Matter 18 4481

(http://iopscience.iop.org/0953-8984/18/19/004)

INSTITUTE OF PHYSICS PUBLISHING JOURNAL OF PHYSICS: CONDENSED MATTER

J. Phys.: Condens. Matter **18** (2006) 4481–4488 doi:10.1088/0953-8984/18/19/004

Liquid droplet spreading with line tension effect

H Fan

School of Mechanical and Aerospace Engineering, Nanyang Technological University, Singapore 639798, Republic of Singapore

E-mail: mhfan@ntu.edu.sg

Received 17 February 2006, in final form 20 March 2006
Published 25 April 2006
Online at stacks.iop.org/JPhysCM/18/4481

Abstract

For a macroscopic liquid droplet, we applied the fluid mechanics to predict its dynamic spreading where the energies associated with volume are dominant (e.g. Shikhmurzaev 1997 *J. Fluid Mech.* **334** 211). When the droplet size is reduced to the sub-millimetre level, the surface energy becomes the dominant factor. If the droplet size is further reduced to the micrometre or sub-micrometre level, the line tension should be included in our theoretical formulation for predicting droplet spreading. In the present paper, we extend the non-equilibrium thermodynamics (Gao *et al* 2000 *Acta Mater.* **48** 863–74) to describe the micrometre or nanometre size droplet spreading on a solid substrate with the line tension effect. Discussion of the stable and unstable equilibrium states is made based on the thermodynamic force expression.

1. Introduction

From the continuum physics point of view, the total energy of condensed matter consists of two parts, namely, the energy associated with the volume and the energy associated with surfaces. When a liquid droplet is large in volume, its dynamic spreading process on a solid surface is characterized by conversion between its gravity potential energy and the kinetic energy of the liquid flow. Rigorous mathematical description is made possible via Navier–Stokes equations (for example, [1]). When the droplet under concern is at the sub-millimetre level, the surface energy dominates the evolution process. Let us have a numerical sense by considering a spherical shaped water droplet. Its volume associated energy can be represented by its gravity potential energy. Its kinematics energy of flow is converted from the potential energy. Therefore, they should be of the same order of magnitude.

$$E_V = mgR = \rho V g R = \frac{4\pi}{3} R^4 \rho g. \tag{1.1}$$

The surface associated energy is estimated as

$$E_S = 4\pi R^2 \gamma. \tag{1.2}$$

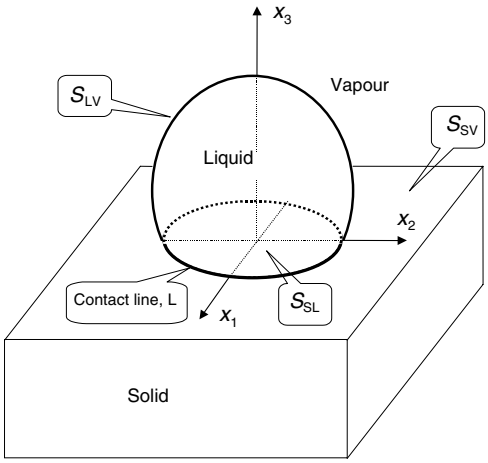

Figure 1. A liquid droplet spreading on a solid.

If we take the physical constants for water, $\gamma = 72 \times 10^{-3}$ J m^{-2} and $\rho = 1000$ kg m^{-3}, and equate the two energies to have the value of R at which the surface energy is on a par with the volume energy, we have

$$R = \sqrt{\frac{3\gamma}{\rho g}} \approx 4 \text{ mm}. \tag{1.3}$$

In other words, when the droplet size is much smaller than 4 mm in radius, the motion is driven by conversion among the surface energies. The conventional fluid mechanics based on Navier–Stokes equations is not capable of describing the droplet evolution. A non-equilibrium thermodynamics framework seems feasible for describing this sub-millimetre droplet spreading process [2]. If the droplet size is further reduced, the so-called line tension should be included in the description of the spreading. Let us make an estimation based on the geometric configuration of figure 1. Assuming a semi-spherical shaped water droplet with its contact line on the solid substrate, we take the surface energy as 72 mJ m^{-2}. The line tension value is not very well documented in the literature. Its experimental values are reported in the range of a few orders of magnitude (from 10^{-10} to 10^{-6} N; see [3]). By setting the surface and line energies on a par, we find the radius of the liquid droplet is in the range of 1 nm–10 μm. We have a dilemma here: on the one hand, the above dimensional analysis needs the droplet to be small so that the line tension prevails in comparison with the surface tension. On the other hand, we have a 'lower bound' of the size of the droplet for meaningful application of continuum physics. In the present study, we assume that the line tension is not at the lower end of its range and the droplet dimension is in the range of continuum physics; otherwise, a discrete approach (say, molecular dynamics) should be employed in study of the present problem.

The line tension effect has been recognized by the researchers in the field of colloid science (for example, [4]). Some recent publications shed light on the research interests in this field. Avyard *et al* [5] extended the liquid bridging solution between two spheres with the line tension effect. Marmur and Krasovisky [6] considered a liquid droplet on a curved solid surface with the line tension effect. More recently, Brinkmanm *et al* [7] studied the stability of liquid channels in the presence of the line tension. Although the above referenced works do not represent a thorough review of this research area, they represent the interests in this field—the

equilibrium state of the liquid droplet with the line tension effect. In the following sections, we would like to turn our attention to the dynamic process of the liquid spreading via a non-equilibrium thermodynamics framework [2, 8], with which the evolution process is directed to lowering the total free energy of the system. Speaking of the system, it should include the volume of the fluid, all the interfaces, and the triple point line (contact line). The free energy should include the contributions from all these sources. However, it is noticed that the volume contribution is negligible for the size of the droplet under consideration. In other words, the spreading evolution is led by the surface and the line energies, rather than the gravity potential energy.

2. Non-equilibrium thermodynamics formulation

Let us consider a vapour/liquid/solid system shown in figure 1. A liquid droplet is placed on a smooth and horizontal solid surface with vapour/liquid, liquid/solid and vapour/solid interfaces that conjoin at a contact line. The solid is assumed not to dissolve or react with the liquid. The interface change and the contact line motion are considered here in terms of thermodynamics formulation. The non-equilibrium thermodynamics requires that the system change is the process of reducing system Gibbs free energy towards its minimum value. For the system of the droplet, we consider the evolution of the interfaces S_{ij} and the motion of contact line driven by the change of the Gibbs free energy, denoted by G hereafter. The free energy consists of the sum of the interface energies among different phases, denoted by U, and the negative work supply W to the system by the external actions. We have

$$G = U - W$$

with

$$U = \gamma_{\mathrm{LV}} A_{\mathrm{LV}} + \gamma_{\mathrm{SV}} A_{\mathrm{SV}} + \gamma_{\mathrm{SL}} A_{\mathrm{SL}} + \tau L \tag{2.1}$$

where γ_{ij} is the specific surface tension and A_{ij} is the area of the interface S_{ij} between phase i and phase j, with phases L, S and V denoting the liquid, the solid and the vapour surrounding the liquid, respectively. The last term in equation (2.1) is the line tension effect, where τ is the line tension and L is the length of the contact line.

From equation (2.1), the free energy change of the vapour/liquid/solid system can be expressed by

$$\delta G = \gamma_{\mathrm{LV}} \delta A_{\mathrm{LV}} + \gamma_{\mathrm{SV}} \delta A_{\mathrm{SV}} + \gamma_{\mathrm{SL}} \delta A_{\mathrm{SL}} + \tau \delta L - \delta W. \tag{2.2}$$

It is seen that the change of the free energy is due to the geometric shape change of the droplet. As there are countless paths of the evolving processes that would reduce the free energy, the free energy by itself is not sufficient to determine the evolution of the vapour/liquid/solid system. We need to relate the geometric change of the liquid/vapour interface and contact line with the thermodynamic forces acting on them. They are the so-called constitutive equations for the evolution.

2.1. Geometric change of the interface and contact line

The area of a surface element is denoted by $\mathrm{d}A$, and the length of a line element of the contact line is denoted by $\mathrm{d}l$. The unit vector normal to the vapour/liquid interface is denoted by $\mathbf{n}$, directing to the vapour phase. The sum of the two principal curvatures of S_{LV} (indicated in figure 1) is given by

$$\kappa = \frac{1}{R_1} + \frac{1}{R_2} \tag{2.3}$$

where R_1 and R_2 are the principal radii of curvature, taken to be positive for a convex surface. On the one hand, associated with the virtual motion, δr_n, the area of the interface S_{LV} varies by

$$\delta A_{\mathrm{LV1}} = \int\int_{S_{\mathrm{LV}}} \kappa \delta r_n \, \mathrm{d}A. \tag{2.4}$$

The integral extends over the interface S_{LV}. On the other hand, associated with the virtual motion of the contact line, δR_{L}, the area of the interface S_{LV} varies by

$$\delta A_{\mathrm{LV2}} = \oint_{\mathrm{L}} \delta R_{\mathrm{L}} \cos\theta \, \mathrm{d}l \tag{2.5}$$

without changing of curvature in equation (2.3).

The areas of the interface S_{SL} and S_{SV} vary by

$$\delta A_{\mathrm{SL}} = \oint_{\mathrm{L}} \delta R_{\mathrm{L}} \, \mathrm{d}l = -\delta A_{\mathrm{SV}}. \tag{2.6}$$

In equation (2.5), θ is the dynamic contact angle at any point along the contact line and the integral extends along the contact line, denoted by L. Last but not least, the change of the contact line is given by

$$\delta L = \oint_{\mathrm{L}} \frac{\delta R_{\mathrm{L}}}{R_{\mathrm{L}}} \, \mathrm{d}l. \tag{2.7}$$

During the evolution process of the contact line and the liquid/vapour interfaces, the virtual motions of S_{LV} at any point on the contact line must be satisfied with the following compatibility condition:

$$\delta r_n = \delta R_{\mathrm{L}} \sin\theta, \qquad \text{on } L.$$

Other constraint conditions, such as no volume change if no evaporation or condensation is assumed, can be applied to the geometric change of the system.

2.2. Driving forces and kinetic laws

Having the aforementioned virtual motions, we can define the thermodynamic force on the liquid/vapour interface, f_{S}, and the force on the contact line, f_{L}. As the free energy decreases with respect to the virtual motions, we have [8]

$$\oint_{\mathrm{L}} f_{\mathrm{L}} \delta R_{\mathrm{L}} \, \mathrm{d}l + \int\int_{S_{\mathrm{LV}}} f_{\mathrm{S}} \delta r_n \, \mathrm{d}A = -\delta G. \tag{2.8}$$

Since the virtual motion δr_n is an arbitrary function of the position on the interface S_{LV} and δR_{L} is also an arbitrary function of the position on the line L, equation (2.8) uniquely defines the quantity f_{S} at every point on the interface S_{LV} and f_{L} at every point along the contact line L. The above-defined thermodynamics force f_{S} has a unit of stress (force/area) and f_{L} has a unit of surface tension (force/length). They are called driving forces of the dynamic system.

Let v_{L} and v_{S}^n be the actual velocity of the contact line L and the interface S_{LV}, respectively. Under the framework of thermodynamics, the actual velocities are taken to be functions of the driving forces. In the present study, the velocity is assumed to be linearly proportional to the driving force (for example, [9]), i.e.

$$v_{\mathrm{L}} = M_{\mathrm{L}} f_{\mathrm{L}} \tag{2.9a}$$

$$v_{\mathrm{S}}^n = M_{\mathrm{S}} f_{\mathrm{S}}. \tag{2.9b}$$

In the above equation, M_{L} and M_{S} are called the *mobilities* of the contact line and the liquid/vapour interface S_{LV}, respectively. These two quantities are used as phenomenological

parameters of the system, to be determined by comparing theoretical predictions with experimental measurements (see [10]). Since the thermodynamics requires that the evolution leads the reduction of the free energy of the system, both M_{L} and M_S are positive. Equations (2.9*a*) and (2.9*b*) are called the kinetic laws for the contact line and the liquid/vapour interface. It should be noted that the kinetic laws (2.9*a*) and (2.9*b*) are linear relations and the velocity at a point only depends on the forces at this point, namely, a local relation. In general, the kinetic laws can be generalized to non-linear and non-local relations if the linear law fails to give a good predication of the experimental result.

3. Motion equations and equilibrium conditions

Noting that the external work change is given by

$$\delta W = \int\int_{S_{\mathrm{LV}}} \Delta p \delta r_n \,\mathrm{d}A, \tag{3.1}$$

where Δp is the pressure difference across the surface S_{LV}, which is the so-called Laplace pressure, we rewrite equation (2.2) as

$$\begin{aligned}\delta G = &\oint_{\mathrm{L}} \gamma_{\mathrm{SL}} \delta R_{\mathrm{L}} \,\mathrm{d}l - \oint_{L} \gamma_{\mathrm{SV}} \delta R_{\mathrm{L}} \,\mathrm{d}l + \oint_{\mathrm{L}} \gamma_{\mathrm{LV}} \delta R_{\mathrm{L}} \cos\theta \,\mathrm{d}l + \oint_{\mathrm{L}} \frac{\tau}{R_{\mathrm{L}}} \delta R_{\mathrm{L}} \,\mathrm{d}l \\ &+ \int\int_{S_{\mathrm{LV}}} \gamma_{\mathrm{LV}} \kappa \delta r_n \,\mathrm{d}A - \int\int_{S_{\mathrm{LV}}} \Delta p \delta r_n \,\mathrm{d}A.\end{aligned} \tag{3.2}$$

A comparison of equations (2.8) and (3.2) gives the expressions of the driving forces

$$f_{\mathrm{L}} = \gamma_{\mathrm{SV}} - \gamma_{\mathrm{SL}} - \gamma_{\mathrm{LV}} \cos\theta - \frac{\tau}{R_{\mathrm{L}}} \tag{3.3a}$$

and

$$f_{\mathrm{S}} = \Delta p - \gamma_{\mathrm{LV}} \kappa. \tag{3.3b}$$

Combination of equations (2.9) and (3.3) leads to

$$v_{\mathrm{L}} = M_{\mathrm{L}} \left(\gamma_{\mathrm{SV}} - \gamma_{\mathrm{SL}} - \gamma_{\mathrm{LV}} \cos\theta - \frac{\tau}{R_{\mathrm{L}}} \right), \qquad \text{for contact line} \tag{3.4a}$$

and

$$v_{\mathrm{S}}^n = M_{\mathrm{S}} (\Delta p - \gamma_{\mathrm{LV}} \kappa), \qquad \text{for liquid/vapour interface.} \tag{3.4b}$$

These nonlinear differential equations govern the motions of the contact line and the liquid/vapour interface during the system evolution. The motions of the contact line and the change of the interfaces depend on the solution of the set of motion equations (3.4) under certain initial-value and boundary conditions (for example [2], where zero line tension was considered). It is worthwhile to mention that the solution of the droplet evolution described via the above thermodynamic frame does not involve the viscosity of the liquid which is associated with the conventional fluid mechanics. The liquid spreading speed is controlled by the new pair of parameters, i.e. the mobility of the surface and the contact line which are determined experimentally [10].

At the end of the evolution process, the system reaches an equilibrium state. At that time, the free energy of the system achieves its minimum value, the liquid/vapour interface shape and contact line position are no longer changing anymore, the contact angle arrives at its static

value, and the driving forces vanish. Setting $f_L = 0$ and $f_S = 0$ in equations (3.3) results in the equilibrium conditions for the contact line and the interface,

$$\gamma_{SV} - \gamma_{SL} - \gamma_{LV}\cos\theta_e - \frac{\tau}{R_L} = 0 \tag{3.5a}$$

$$\Delta p - \gamma_{LV}\kappa = 0. \tag{3.5b}$$

Equation (3.5*a*) is the modified Young's equation with the line tension effect, and equation (3.5*b*) is the well known Laplace's equation. In the equation, θ_e is the equilibrium contact angle.

4. Discussions

For a full scale numerical simulation of the droplet spreading on a solid surface, readers need to read Gao *et al* [2] and Suo [8] for the detailed weak statement of the problem, where no line tension was considered ($\tau = 0$). Here, we make a simplified numerical simulation by assuming the droplet shape as a cap of a sphere. This assumption reduces the number of generalized coordinates to one, i.e. the radius of the contact line. As the thermodynamics force in equation (3.3*a*) includes the line tension effect, we can expect that the spreading speed is reduced as the line tension increases. The evolution of the droplet can be simulated by

$$\delta(R_L/R_*) = \left(\cos\theta_0 - \cos\theta - \frac{\tau}{\gamma_{LV}R_L}\right)\delta(t/t_0) \qquad \text{for the contact line}$$

and

$$\delta(r_n/R_*) = \chi\left(\frac{R_*}{\gamma_{LV}}\Delta p - R_*\kappa\right)\delta(t/t_0) \qquad \text{for the liquid/vapour interface,}$$

where $t_0 = \frac{R_*}{M_L\gamma_{LV}}$, $\chi = \frac{M_S}{R_*M_L}$ and θ_0 is the equilibrium contact angle in the absence of the line tension. A parameter, $R_* = \sqrt[3]{V}$ (V is the volume of the liquid droplet), is selected for the normalization purpose. The numerical iteration, which simulates the elevation of the droplet shape, can be carried out, after we specify the non-dimensional parameters (t_0 and χ) and an initial shape of the droplet (e.g. [2]).

An important issue comes up with the 'initial values of contact angle'. Examining the thermodynamics force acting on the contact line, equation (3.3*a*)

$$f_L = \gamma_{SV} - \gamma_{SL} - \gamma_{LV}\cos\theta - \frac{\tau}{R_L},$$

we notice that the force is monotonically decreasing when the line tension term is absent. In other words, there is only one equilibrium solution for

$$\gamma_{LV}\cos\theta_0 = \gamma_{SV} - \gamma_{SL}. \tag{4.1}$$

However, when the line tension term is included in the force equation, there are two roots for the equilibrium condition. The equilibrium condition, equation (3.5*a*), with the help of equation (4.1), is written as

$$\cos\theta_0 - \cos\theta = \frac{\tau}{\gamma_{LV}R_L}, \qquad \text{with } 0 < \theta_0 \leqslant \pi. \tag{4.2}$$

The first root to equation (4.2) is the modification of the equilibrium contact angle under the zero line tension condition, which is close to θ_0; the second solution is close to $\theta = \pi$.

Although the numerical solutions can be easily obtained, we prefer to have the analytical approximated solutions which may shed more light on the problem. Having assumed that the

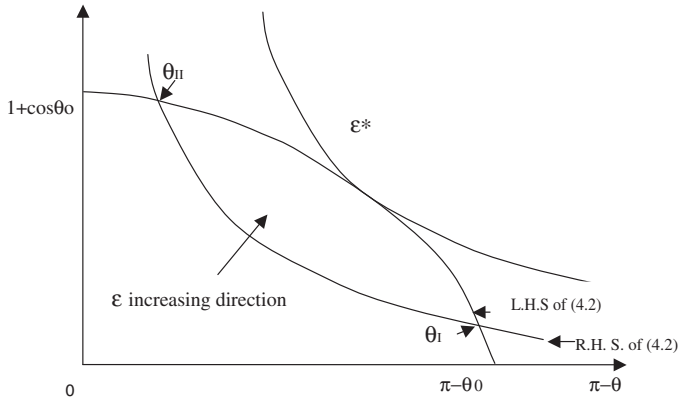

Figure 2. Schematic display of the solution of equation (4.2).

droplet shape is approximated by a partial sphere, we can write the volume of the droplet in terms of contact angle and radius of the sphere, i.e.

$$V = R^3 F(\theta) = \frac{\pi}{6} R^3 (1 - \cos\theta)(3\sin^2\theta + (1 - \cos\theta)^2).$$

By noting that $R_{\mathrm{L}} = R\sin\theta$, we rewrite equation (4.2) as

$$(\cos\theta_0 - \cos\theta)\sin\theta = \varepsilon\sqrt[3]{F(\theta)} \tag{4.3}$$

where $\varepsilon = \frac{\tau}{\gamma_{\mathrm{LV}}\sqrt[3]{V}} = \frac{\tau}{\gamma_{\mathrm{LV}} R_*}$ is a small parameter in most cases. It is straightforward to have the perturbed solutions as

$$\theta_{\mathrm{I}} = \theta_0 + \varepsilon\sqrt[3]{F(\theta_0)}\Big/\sin^2\theta_0 + \mathrm{O}(\varepsilon^2) \tag{4.4a}$$

$$\theta_{\mathrm{II}} = \pi - \varepsilon\sqrt[3]{\frac{4\pi}{3}}/(1 + \cos\theta_0) + \mathrm{O}(\varepsilon^2). \tag{4.4b}$$

Equation (4.4*a*) is a stable solution, which should be observed in experimental measurement. Equation (4.4*b*) is an unstable solution, which will not be observed in the experimental test.

The final equilibrium state of the droplet depends on the initial condition. We will see the following situations.

(1) $\theta_{\mathrm{initial}} > \theta_{\mathrm{II}}$; the contact angle evolves towards π.
(2) $\theta_{\mathrm{II}} > \theta_{\mathrm{initial}} > \theta_{\mathrm{I}}$; the contact angle evolves towards θ_{I}.
(3) $\theta_{\mathrm{initial}} < \theta_{\mathrm{I}}$; the contact angle evolves towards θ_{I}.

It is interesting to notice that although the two solutions are obtained from the equilibrium equation (4.3), explaining the stability of the solutions involves the dynamic process of the droplet spreading. It is also seen that there is a critical value of ε^* from observation of figure 2. Equation (4.3) has no solution with $\varepsilon > \varepsilon^*$, which means that we can only expect the liquid droplet in a spherical shape with contact angle of π. Widom [11] reached a similar conclusion based on an equilibrium study (noting that the definition of the contact angle in his paper is different from ours). With the help of the energy consideration, he drew the same conclusion as above for the positive line tension force. It should be mentioned that his study also included the solution and discussion of the negative line tension case, which is of great interest from an experimental point of view. Examining our solution equation (4.4), we find that for the negative line tension ($\varepsilon < 0$) the second root given by (4.4*b*) does not fit the physical reality (the equilibrium contact angle must be in the range of $0 \leqslant \theta \leqslant \pi$). In other words, there

is only one equilibrium contact angle for negative line tension cases, which is consistent with Widom's figure 2. However, we would like to emphasize that the present analytical model not only predicts the stable and unstable equilibrium contact angles, but also provides the dynamic evolution history from the unstable towards the stable situation.

References

[1] Shikhmurzaev Y D 1997 *J. Fluid Mech.* **334** 211
[2] Gao Y X, Fan H and Xiao Z 2000 *Acta Mater.* **48** 863–74
[3] Kralchevsky P A and Nagayama K 2001 *Particles at Fluid Interfaces and Membranes* (Amsterdam: Elsevier)
[4] de Gennes P G 1985 *Rev. Mod. Phys.* **57** 827
[5] Aveyard R, Clint J H, Paunov V N and Ness D 1999 *Phys. Chem. Chem. Phys.* **1** 155–63
[6] Marmur A and Krasoviski B 2002 *Langmuir* **18** 8919–23
[7] Brinkmanm M, Kierfeld J and Lipowsky R 2005 *J. Phys.: Condens. Matter* **17** 2349–64
[8] Suo Z 1997 *Adv. Mech.* **33** 193
[9] de Groot S R and Mazur P 1962 *Non-Equilibrium Thermodynamics* (New York: North-Holland)
[10] Fan H, Gao Y X and Huang X Y 2001 *Phys. Fluids* **13** 1615–23
[11] Widom B 1995 *J. Phys. Chem.* **99** 2803–6